

# Life Cycle Assessment of Fusion Welding Processes—A Case Study of Resistance Spot Welding Versus Laser Beam Welding

Andreas Pittner\* and Michael Rethmeier

The high amount of resource consumption of fusion welding processes offers the potential to reduce their environmental impact. While the driving forces are known from a qualitative perspective, the quantitative assessment of the crucial parameters is not a trivial task. Therefore, herein, a welding-specific methodology to utilize life cycle assessment as a tool for evaluating the environmental impact of fusion welding processes is presented. In this context, two welding processes, resistance spot welding and laser beam welding, are analyzed for two different use cases. These comprise the welding of shear test specimens and a cap profile made of electrogalvanized sheets of DC 05 + ZE (1.0312) as representative of an automotive application. For both welding processes, the main influences on the resulting environmental impact categories are evaluated and compared. The requirements for ecological efficient welding processes are discussed and implemented.

It is worth noticing that life cycle assessment of fusion welding processes has become well established during the last decade as shown by the author for different gas metal arc welding (GMAW) and laser beam-welding (LBW) processes.<sup>[9–13]</sup> Other authors, that is, Metha,<sup>[14]</sup> were analyzing different welding processes like GMAW, friction stir welding (FSW), and LBW with respect to their influencing parameters of process design on the environmental impact. Huang<sup>[15]</sup> showed that the carbon efficiency of LBW is driven by the process parameters but also governed by external equipment conditions such as the laser source cooling device. As a result, the idle mode during laser operation must be reduced to gain a better overall efficiency

that yields a less destructive carbon footprint. In this context, Kaierle<sup>[16]</sup> could also show that LBW is one of the most resource-efficient welding processes since no filler material is used and the seam shape (nearly parallel flanges in comparison to V-groove shapes for GMAW processes) requires less metal to be molten. Nevertheless, due to the low efficiencies in energy consumption of the laser equipment (laser source), the process requires high utilization to run economically and ecologically efficient. A more material focused view on environmental impact assessment of LBW of thick plates was done by Yilbas<sup>[17]</sup> who analyzed the effect of different alloys ranging from Inconel 625, AISI 304 to Ti6Al4V. It was found that the environmental impact depends on the base material selection and is maximal for Inconel 625.

Because arc welding is the most spread welding technology in industry, many research works exist dealing with a corresponding life cycle assessment for such processes. In this relation, Favi<sup>[18]</sup> compared a wide range of arc welding processes. Based on a functional unit of 1 m of weld seam length, the welding of 25 mm thick plates of mild steel was considered. The life cycle inventory (LCI) as well as impact assessment was supported by a framework for data collection to easily implement the corresponding results in the project documentation.


In addition, Sangwan<sup>[19]</sup> performed a life cycle assessment of different arc and gas welding processes. He stated that the inventory in terms of the consumption of resources like electrical energy or consumables is different for each process and recommends assessing the environmental impact for a particular welding process individually. However, pre- and post-processes or external equipment conditions that characterize a welding technology, rather than the discrete welding process, were not

## 1. Introduction

Manufacturing processes contribute to the overall environmental impact of industrial products and therefore need to be analyzed with respect to their ecological footprint.<sup>[1]</sup> Fusion welding as a relevant representative of manufacturing processes accounts to the overall environmental impact of numerous industry sectors within a global context.<sup>[2]</sup> The fusion welding processes are characterized by a significant amount of energy and resource consumption. Consequently, the demand for a process related life cycle assessment to evaluate the environmental burdens is widely addressed involving application ranging from the automotive industry<sup>[3–5]</sup> to ship-building<sup>[6,7]</sup> or additive manufacturing.<sup>[8]</sup>

A. Pittner, M. Rethmeier  
Devision Welding Technology  
Bundesanstalt für Materialforschung und –prüfung  
Unter den Eichen 87, 12205 Berlin, Germany  
E-mail: andreas.pittner@bam.de

M. Rethmeier  
Institute of Machine Tools and Factory Management  
Technical University Berlin  
Pascalstr. 8-9, 10587 Berlin, Germany

 The ORCID identification number(s) for the author(s) of this article can be found under <https://doi.org/10.1002/adem.202101343>.

© 2022 The Authors. Advanced Engineering Materials published by Wiley-VCH GmbH. This is an open access article under the terms of the Creative Commons Attribution License, which permits use, distribution and reproduction in any medium, provided the original work is properly cited.

DOI: 10.1002/adem.202101343

regarded but might influence the overall resource demand as shown by Huang et al. and Kaieler et al.<sup>[15,16]</sup>

Supplement to fusion welding processes, Bevilacqua<sup>[20]</sup> evaluated the sustainability of FSW of aluminum AA 5575 sheets. In his work, the environmental impact for different process parameter settings was determined. The function unit was defined as a sound weld fulfilling the mechanical properties as requested by the standards. In this context, Shrivastava<sup>[21]</sup> provided a comparative life cycle assessment of FSW and GMAW of aluminum. He argues that the reduced energy consumption of FSW in comparison to GMAW is known qualitatively but the quantitative evaluation of the environmental impact requires energy and resource consumption measurements during the process. Moreover, he showed that the functional unit must account for the different characteristics of the welding processes to compare them equitably. Here, the similar ultimate strength of the resulting joint was defined as functional unit that corresponds to the fulfillment of the technological requirements of the joint, which results in different sheet thicknesses correspondingly.

It can be stated that most research articles focus on the evaluation of the significant influencing parameters on the environmental impact categories for distinct welding processes or process comparisons and subsequent sensitivity studies.<sup>[22,23]</sup> One crucial aspect is the seamless availability of process related data sets that govern the inventory of consumed energy and resources. Therefore, Epping<sup>[24]</sup> promoted the potential of automated welding processes with data recording to provide the basis for life cycle assessments for small and medium enterprises. The integration of life cycle assessment within the weld planning and production chain utilizing a data platform is shown by Favi.<sup>[25]</sup>

Summarizing the literature survey, it can be concluded that life cycle assessment has become a standard tool in manufacturing technology from a plant design perspective<sup>[26]</sup> comprising the analyses of other production processes such as cutting and turning<sup>[27]</sup> or even certifying entire production-oriented companies.<sup>[28]</sup> The evaluation of the environmental impact of welding processes is obtained on basis of the individual amount of consumed electrical energy and resources, which requires corresponding data acquisition and handling during the processes. Furthermore, if the environmental impact of different processes is of interest, the performed assessment must be equitable for each technology by defining an appropriate functional unit. However, while the evaluation of influencing factors on the environmental impact is straightforward for a discrete welding process, it might be different, if the energy and resource consumption of pre- and post-processes has to be considered as well as the influence of external equipment within a factory context, that is, laser idle times, cooling devices, etc. This means, that the entire welding manufacturing chain with specific technology requirements has to be accounted for to let life cycle assessment be a comparable and reliable decision tool for welding process design.

Based on the findings aforementioned, the goal of the present article is to provide a systematic approach to analyze two different welding technologies that are relevant for the automotive industry and have not been studied so far referring to a direct comparison. Exemplarily for resistance spot welding (RSW) and LBW of low-alloyed electrogalvanized steel sheets (DC 05 + ZE), the governing process characteristics on the environmental impact

categories are determined for two different case studies. These comprise the welding of shear test specimens to provide process characteristics that yield fusion welds with comparable mechanical properties. The findings are transferred onto a more complex welding application from automotive industry that includes the welding of 1 m of a cap profile as functional unit. It is shown that within a factory context, the technology-dependent needs for electrical energy, base material, or other consumables as well as external equipment conditions have the strongest influence on the overall resource consumption and cannot be derived from the discrete processes directly.

## 2. Life Cycle Impact Assessment of Welding Processes

Life cycle impact assessment (LCIA) is a standardized method in accordance with international standards<sup>[29,30]</sup> as well as corresponding reference literature<sup>[31]</sup> and used to evaluate the environmental impact of a product system during its life cycle beginning from the raw material extraction and ending with its recycling (cradle-grave-approach).

According to the ISO standard, the methodology includes four major phases. These are the goal and scope definition, the LCI analyses, the LCIA, and the interpretation of the results. Since there exists a strong bidirectional relationship between all the phases, they are executed in an iterative manner.

Concerning the goal of the performed life cycle assessment, the current study aims to clarify the environmental impact governed by different inputs and outputs for two fusion welding processes widely used in automotive industry. The differences in environmental impact are expected to provide necessary information for an economically efficient welding process selection. Moreover, the scope of the study focuses on the welding processes, in particular the life cycle stages of material acquisition that includes the extraction of raw material and subsequent material processing during welding, the manufacturing phase which is given by the welding process itself and the waste management. The definition of the scope governs the setup of the LCIA system determined by a proper selection of system boundaries. Exemplarily for the welding processes under investigation, LBW and RSW, the corresponding LCIA system boundary is shown in **Figure 1**. As already shown by Sproesser et al.,<sup>[10–12]</sup> the relevant input flows to be considered for the LCIA model of welding processes are the base material consumption (steel sheets), the consumed electrical energy, compressed air, process gases, and protection glasses in case of LBW as well as needed electrode caps for the RSW process. Moreover, the output flows are given by the wear of protection glasses and the wear of electrode caps. In this context, it must be noticed that the life cycle assessment of welding processes spans from the raw material extraction and ends with the finished product leaving the factory gate. This cradle-to-gate approach is common if technology focused life cycle assessments are of interest.<sup>[31]</sup>

All analyses are done with respect to a predefined functional unit that quantifies the use of the assessed product system, which includes the implementation of a certain function, kilogram of product mass or piece, etc. The product system must include all relevant input and output flows that were used for setup of

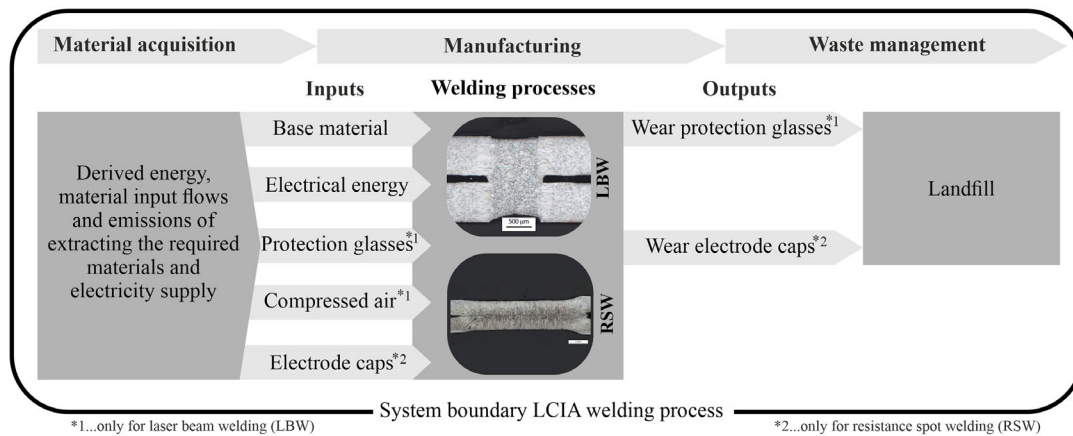


**Figure 1.** Definition of system boundary during life cycle impact assessment (LCIA) for laser beam welding and resistance spot welding in reference with the work by Sproesser et al.<sup>[10,11]</sup>

the life cycle model (Figure 1). In case of welding, the function of the product system is given by the resulting technological properties, that is, strength of the resulting weld seam or material properties within the weld metal and heat-affected zone. Furthermore, the functional unit is defined by normalizing the welding process and allowing a subsequent upscaling and comparison of different welding processes of the same class.

In this case, the functional unit contains the welding of shear test specimens made of electrogalvanized 0.8 mm thick metal sheets of DC 05 + ZE as illustrated in **Figure 2** and **3**.

The environmental impact assessment method can be understood as a set of LCIA impact categories that are expressed in terms of emissions to the environment.<sup>[32,33]</sup> Here, the Centrum voor Milieukunde of University of Leiden-impact

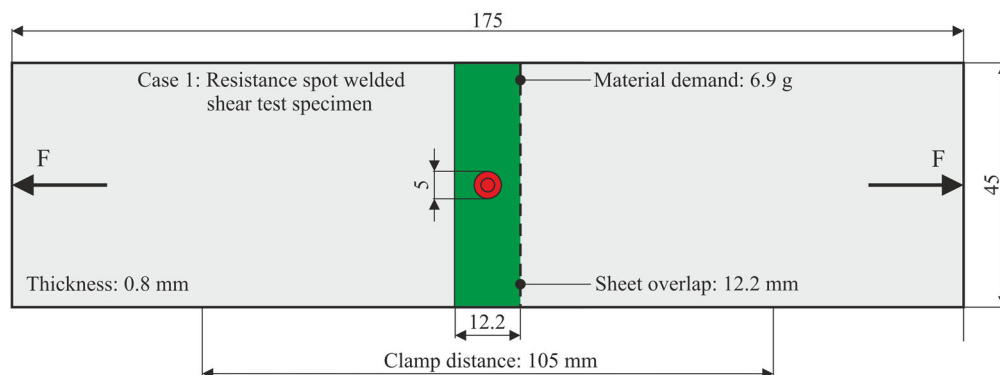


**Figure 2.** Geometry of the shear test specimens used for the resistance spot-welding experiments referring to DIN EN ISO 14273; F indicates the direction of load.

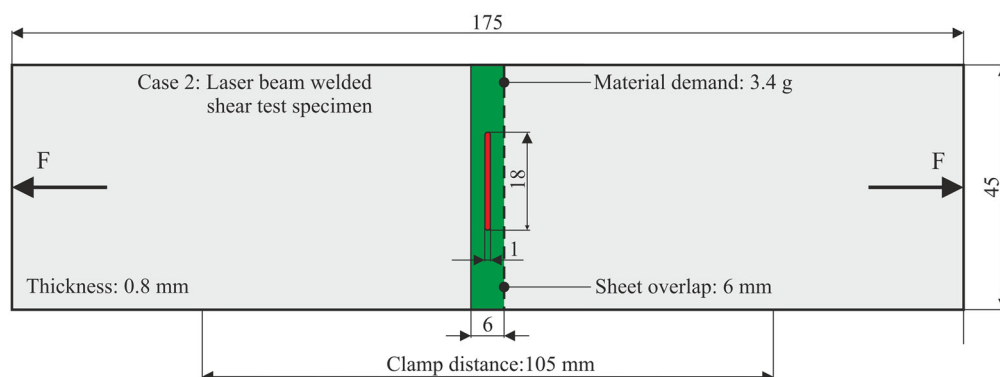


**Figure 3.** Geometry of the shear test specimens used for the laser beam-welding experiments referring to DIN EN ISO 14273; F indicates the direction of load.

assessment (CML-IA) baseline method as a midpoint approach was used on basis of a physical allocation method since the physical values are assumed to reflect the main characteristics of the product. The normalization and weighting sets were selected in accordance with the world-2000 database. The CML impact method has been developed by the centre for environmental studies (CML) of the University of Leiden<sup>[34]</sup> and offers a decision tool for life cycle assessment referring to DIN ISO 14 040.<sup>[29,30]</sup> In this context, the CML method includes the following impact categories: 1) Acidification (acidification potential [AP]—average Europe). 2) Climate change (global warming potential [GWP] 100 years). 3) Depletion of abiotic resources (depletion of abiotic resources—elements, ultimate reserves). 4) Ecotoxicity (freshwater, marine aquatic and terrestrial ecotoxicity). 5) Eutrophication. 6) Human toxicity. 7) Ozone layer depletion. 8) Photochemical oxidation

For fusion welding processes, a reduced set of impact categories as proposed by the World Steel Association<sup>[35]</sup> is appropriate and well established.<sup>[9]</sup> These include the GWP, the eutrophication potential (EP), AP, and the photochemical ozone creation potential (POCP). GWP (100 years, in kilogram of carbon dioxide equivalent) evaluates the long-term contribution of a substance to climate change. EP (in kilogram phosphate equivalent) describes the impact from the macronutrient's nitrogen and phosphorus in bioavailable forms on aquatic and terrestrial ecosystems, affecting undesired biomass production. AP (in sulphur dioxide equivalent) accounts for the impacts from acidification generated by the emission of airborne acidifying chemicals. Acidification refers to processes that increase the acidity of water and soil systems by hydrogen ion concentration. The POCP (in kilogram ethene equivalent), which rates the creation of ozone, is also known as summer smog.<sup>[31]</sup> In this work, openLCA<sup>[36]</sup> that implements the GaBi database (Version 2016, SP30)<sup>[37]</sup> is used as software package for the LCIA modelling discussed earlier. The detailed inventory analyses as well as environmental impact assessment are presented in the subsequent chapters.

### 3. Experimental Section

#### 3.1. RSW and LBW of Shear Test Specimens

The main goal of the current study is to compare the environmental impact of RSW versus LBW by means of a life cycle assessment. As a first step, a functional unit must be defined that allows an equitably comparison of both the welding processes and a subsequent upscaling to real use cases. In this context, the functional unit was governed by technological criteria regarding the functionality and integrity of the weld. More specifically this implies to realize a sound fusion weld with both the processes under investigation that yield similar strength

**Table 2.** Process parameters used for resistance spot welding with a sheet overlap of 12 mm.

	Electrode force [kN] <sup>a)</sup>	Current [kA]	Voltage [V]	Welding time [ms]	Squeeze time [ms]	Hold time [ms]	Process time [s]
AC	2.5	8.2	1	260	200	200	1.5
MF-DC	2.5	7.8	1	260	200	200	1.5
DC							

<sup>a)</sup>The geometry of the shear test specimens used for the LBW experiments are depicted in Figure 3. The sheet overlap was chosen based on the design principles provided by DVS 3203-4<sup>[40]</sup> and the requirements of a stable LBW process.

characteristics of the weld. For this purpose, shear tests in accordance with DIN EN ISO 14 273 were executed and the minimum axial force to be reached was set to 4 kN. The mechanical properties and the chemical composition of the corresponding electrogalvanized steel sheets made of DC 05 + ZE are listed in **Table 1**.

The geometry of the shear test specimens corresponded to DIN EN ISO 14 273. Exemplarily for the RSW process, the geometry of the shear test specimen is shown in Figure 2. The overlap between both steel sheets was set to 12.2 mm, which agreed with the technical specifications after DVS 2902-3 (Table 3.3)<sup>[38]</sup> and allowed realizing a spot diameter of about 5 mm. This value was slightly above the minimum spot diameter after DVS 2902-3<sup>[38]</sup> or SEP 1220-2<sup>[39]</sup> that suggested a spot diameter of  $d_{\min} = 5\sqrt{t}$  with  $t$  being the sheet thickness as lower quality limit.

The process parameters for the RSW experiments are listed in **Table 2**. Two electrical conditions, the alternating current (AC) as well as the mid-frequency direct current (MF-DC), were used. The welding equipment included a Dalex MPS 15 043 (AC) and Bosch PSI 6300 (MF-DC) as power source control acting together with a servo-electrical C-type spot-welding gun from SWAC. Furthermore, standard electrodes of type F16 flattened after ISO 5821 were utilized. The welding current was set to values of 200 A below the spatter limit (higher quality limit) in dependence of the remaining process parameters and in agreement with SEP 1202-2.<sup>[39]</sup>

The LBW experiments were done with a Trumpf TrueDisk 6001 as beam source. Considering a fiber diameter of 100 microns, a Scansonic Remote Laser Welding-Adaptive (RLW-A) with 500 mm optical length and a Trumpf programmable focus optics (PFO) 3D-2 with 450 mm optical length were chosen as laser optics with integrated scanning capabilities. The entire process parameter set is listed in **Table 3**.

#### 3.2. RSW and LBW of an Automotive Cap Profile

In addition to the shear test specimens, the experimental methodology was scaled up to a real industrial use case that covered

**Table 1.** Mechanical properties and chemical composition of the used electrogalvanized sheets made of DC 05 + ZE (1.0312) in agreement with DIN EN 10152:2017.

Mechanical properties			Chemical composition				
Yield strength [N mm <sup>-2</sup> ]	Ultimate strength [N mm <sup>-2</sup> ]	Elongation at fracture A80 [%] min.	C [wt%]	P [wt%]	S [wt%]	Mn [wt%]	Fe [wt%]
180	270–330	39	<0.06	<0.025	<0.025	<0.35	Balanced

**Table 3.** Process parameters used for laser beam welding with a sheet overlap of 6 mm.

Laser power [kW]	Welding velocity [[m] [min] <sup>-1</sup> ]	Focus position [mm]	Spot diameter [mm]	Joint gap [mm]
4	6	0	0.6	0.12

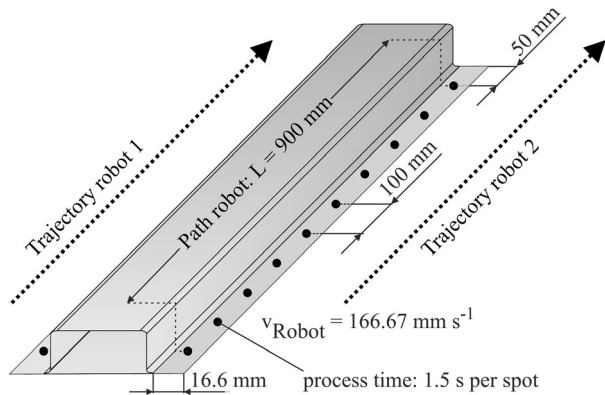


**Figure 4.** Design of resistance spot-welding process for the cap profile based on the process parameter settings of the shear test specimens; drawn not in scale.

the welding of a cap profile with a length of 1 m representing the functional unit as illustrated in **Figure 4**. Like the shear test specimens, the cap profiles were made of electrogalvanized DC 05 + ZE steel sheets with a thickness of 0.8 mm and flange width of 16.6 mm in accordance with DVS 2902-3 (Table 3.3).<sup>[38]</sup>

For the RSW in AC and mid-frequency DC mode, the process parameters were taken from the shear test specimens as listed in Table 2. The welding was done simultaneously with two robots of class Kuka KR120 (120 kg carry load) as indicated by the two trajectories in **Figure 4**. The net power consumption for one robot was 3 kW. The total time of moving per robot was defined by its approach time of 1.1 s, the leaving time of 0.4 s, and the time needed for moving along the path of 900 mm length with a speed of 10 m min<sup>-1</sup> or 166.67 mm s<sup>-1</sup> of 5.4 s. This accumulated to a total time of moving of 6.9 s. Moreover, the welding time for a

single spot was set to  $t_{\text{weld}} = 0.26$  s as listed in Table 2. The process time to manufacture a weld spot including the squeeze time, heating and welding time, as well as the subsequent hold time was 1.5 s. To form the ten spots per robot, this required 15 s for realizing the weld spots and yielded in a total time demand for manufacturing the cap profile of 21.9 s per robot whereas the time for the welding only accounted for 2.6 s. This corresponded to a total share of 12% on the total manufacturing time per robot.

The LBW of the cap profile involved the 20 short step welds each with a length of 18 mm as shown in **Figure 5**. The process parameters and setup corresponded to those obtained during the welding of the shear test specimens (Table 3). Contrary to the RSW, only one robot of class Kuka KR30 with a net power consumption of 1.3 kW was utilized.

Furthermore, two different experimental scenarios were considered. As illustrated in **Figure 5a**, the scanner optics RLW-A was utilized to perform the 20 step welds sequentially by moving the beam between both the flanges. The total length of the robot moving path was 900 mm. However, the moving speed was not constant but set to a welding velocity of  $v_{\text{weld}} = 100$  mm s<sup>-1</sup> and a moving velocity between the welds of  $v_{\text{idle}} = 150$  mm s<sup>-1</sup>. For a distance between the laser welds of 80 mm, this equaled to a length of 720 mm that required 4.8 s to pass. Assuming an approach time of 1.1 s and a leaving time of 0.4 s, the total time of moving without welding (idle time) was 6.3 s. The time for welding the step welds was 3.6 s but the robot moving time during welding was only 1.8 s since the welds at both the flanges were assumed to be realized simultaneously. This summed up to total time for manufacturing the cap profile of 8.1 s whereas the share of the welding process on the overall time demand was 44%.

In addition, a second test case was analyzed as schematically shown in **Figure 5b**. Here, the scanner optics PFO 3D-2 was applied that enabled a fully simultaneous “on-the-fly” welding of the 20 step welds. In this context, the path of the robot movement could be reduced to 600 mm while defining a constant moving velocity of the robot of  $v_{\text{moving}} = 150$  mm s<sup>-1</sup>. Again, taking an approach time of 1.1 s and a leaving time of 0.4 s into account, the total time of manufacturing was 5.5 s. However, the programmable scanner optics allowed a flexible path design of the laser beam so that the local welding velocity corresponded to the parameter settings given in Table 3 because the welding

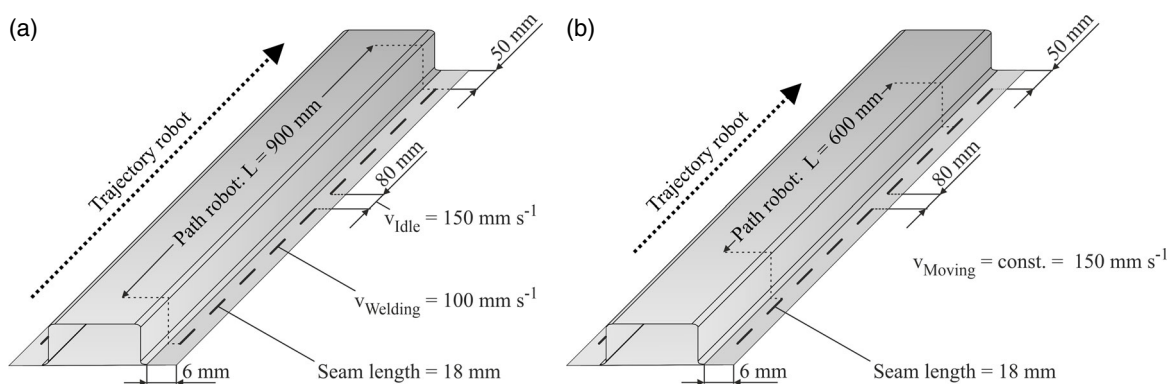


**Figure 5.** Design of laser beam-welding process for the cap profile; a) RLW-A optics from Scansonic as scanning optic and welding sequentially and b) utilizing a PFO 3D-2 scanner optics from Trumpf enabling an “on-the-fly” welding. The process parameter settings are based on the shear test specimens of Table 3; drawn not in scale.

**Table 4.** Input flows for LCIA model representing the resistance spot–welding process.

Functional unit I (FU I): Fusion welding (RSW/LBW) of a shear test specimen resisting an axial force of minimum 4 kN.		Functional unit II (FU II): Fusion welding (RSW/LBW) of a 1 m cap profile with a cover plate by 20 spots.
Inputs	Outputs	
Electrical energy	Process-specific material consumption	Wear electrode caps
Power source and control for forming a single weld spot (net heat input)	0.8 mm thick DC 05 + ZE sheets with an overlap of 12.2 mm and width of 45 mm (FU I: shear test specimens) and a flange width of 16.6 mm and a length of 2 × 1 m for the cap profile (FU II)	Lifetime of cap: 1000 spots Production and waste Recycling rate: 50%
Operation servo-electrical weld gun		
Cooling weld gun (electrode caps)		

velocity was uncoupled from the robot moving. With this regards, the welding time for realizing the 20 welds was 3.6 s that corresponded to an idle time of  $1.5\text{ s} + 0.4\text{ s} = 1.9\text{ s}$  and a share of 65.5 % of the total manufacturing time.

### 3.3. Setup of LCIA Process Model

The general methodology to setup the LCIA process model was described in Section 2. The implementation was done using the opensource software package openLCA Version 1.10.3.

In **Table 4**, the corresponding input flows and outputs are listed for the RSW processes that include both the functional units: the RSW of shear test specimens with a specified shear strength as well as the RSW of a cap profile as a representative for an automotive application that are defined as reference product flows.

For the electricity input flow, the German grid mix was assumed by using the following data provider specifications from GaBi database: electricity grid mix, consumption mix, at consumer, AC, technology mix, <1 kV. <sup>[41]</sup>

The process-specific material consumption of DC 05 + ZE steel sheets depends on the overlap length and flange width. The corresponding data provider was defined accordingly: steel sheet electrogalvanized, production mix, at plant, blast furnace route, thickness between 0.3 and 3 mm, typical width between 600 and 2100 mm, global average. <sup>[42]</sup>

The wear of the electrode caps was evaluated by assuming a lifetime of 1000 spots. The electrode caps were made of copper that yielded the subsequent input flow specification as global average: copper mix (99 999% from electrolysis), consumption mix, to consumer. <sup>[43]</sup>

For the LBW experiments, the relevant inputs and outputs to the LCIA model are shown in **Table 5**. The input flows of electrical energy<sup>[41]</sup> and process-specific material consumptions<sup>[42]</sup> were set in accordance with the RSW process. The input flow for compressed air was defined as follows as European average (EU-28): compressed air; 7 bar, high efficiency; production mix, at plant; low electricity consumption. <sup>[44]</sup> In addition, the wear of the protection glasses was considered by an appropriate flow of valuable substances averaged for the EU-28: float flat glass; cut, Pilkington process, from sand and soda ash; production mix, at plant; 23% cullet. <sup>[45]</sup>

The corresponding product systems were built as system processes with a cutoff of 0.1.

## 4. Results and Discussion

### 4.1. Comparison of RSW and LBW of Shear Test Specimens

The welding experiments of the functional unit I are done to obtain comparable technological properties of the welded specimens independent of the welding processes used.

For the RSW experiments, the metallographic analyses showed no cracks or other irregularities as proved by **Figure 6**. Moreover, the resulting spot diameter is about 5.4 mm for the AC mode and 5.1 mm for the MF-DC mode.

Correspondingly, the macrosection as well as the top view of the weld seam for the laser beam–welded specimens is depicted in **Figure 7**. Again, no irregularities are visible so that the found process parameters are validated.

To guarantee comparable mechanical properties of the functional unit I for both the welding processes, the maximum

**Table 5.** Input flows for LCIA model representing laser beam–welding process.

Functional unit I (FU I): Fusion welding (RSW/LBW) of a shear test specimen resisting an axial force of minimum 4 kN.		Functional unit II (FU II): Fusion welding (RSW/LBW) of a 1 m cap profile with a cover plate by 20 spots/welds.	
Inputs	Outputs		
Electrical energy	Process specific material consumption	Compressed air	Wear protection glasses
Laser source and control for forming a weld (net heat input)	0.8 mm thick DC 05 + ZE sheets with an overlap of 6 mm and width of 45 mm (FU I: shear test specimens) and a flange width of 6 mm and a length of 2 × 1 m for the cap profile (FU II)	Cross jet to protect laser optic 1800 L min <sup>-1</sup> with 0.5 s preflow time	Exchange routine every 2 weeks <sup>a)</sup> Production and 100% waste
Cooling laser source			
Cooling laser optic			

<sup>a)</sup>Change every 2 weeks assuming a production scenario of 6 days week<sup>-1</sup>, 8 h day<sup>-1</sup> shift, 30 s cycle time for 20 welds.

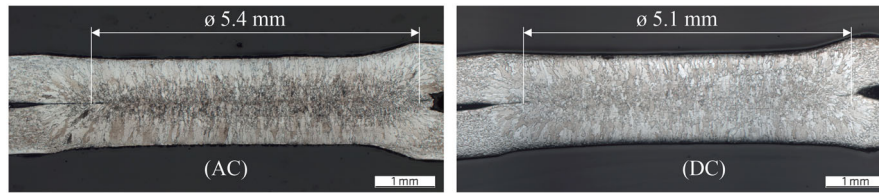


**Figure 6.** Macrosection for AC mode (left) and for DC mode (right) for the resistance spot welded shear test specimens.

occurring axial force during the shear tests should be in the same range and above 4 kN. Therefore, based on the used spot diameter for the AC and DC mode, a corresponding seam length of the laser beam weld had to be found that yields similar force values or strength characteristics, respectively. The results of the shear tests (compare Figure 2 and 3) for the resistance spot-welded specimens with a spot diameter of 5.1–5.4 mm and corresponding laser beam-welded specimens are shown in **Figure 8**. The length of the laser beam welds was found iteratively and was set to 18 mm. Referring to a maximal occurring average axial force of about 4.1 kN for the resistance spot-welded specimens and 4.9 kN for the laser beam-welded ones, both welding technologies can be evaluated as technological comparable, and the defined functional unit is validated as technological criterion. Moreover, the defined seam length of 18 mm for the laser beam welds yields maximum shear forces that are up to 20% higher than those of the resistance spot weld. Consequently, this could lead to the assumption of reducing the laser welded seam length accordingly. However, this would mainly govern the total process time and the associated consumption of electrical energy and compressed air.

## 4.2. Life Cycle Inventory of Shear Test Specimens

### 4.2.1. Resistance Spot Welding

The electrical energy consumption is governed by the required energy of the welding power source and control to form an appropriate spot weld. Furthermore, the servo-electrical weld gun needs electrical energy for operation. In this context, a total process time of the C-gun of 1.5 s was measured whereas the weld time was 0.26 s. In addition, the cooling of the electrode caps must be considered. A detailed listing of calculated inventory is listed later:

*The Total Amount of Electricity to Form a Spot:* Welding Process (MF-DC): 1) Current (averaged 3 measurements): 7785 A. 2) Voltage (averaged three measurements): 0.99 V. 3) Weld time (predefined): 0.26 s. 4) Resulting energy input at the spot:  $7785 \text{ A} \times 0.99 \text{ V} \times 0.26 \text{ s} = 2004 \text{ J}$ .



**Figure 7.** Macrosection (left) and top view (right) of the weld seam for the laser beam-welded shear test specimens.

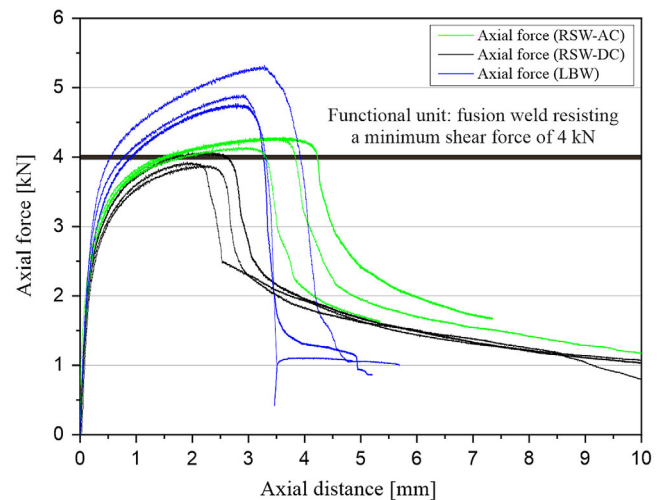


**Figure 8.** Results of shear test for the resistance spot- and laser beam-welded specimens.

The resulting power demand to form the spot is 7708 kW. It is known that up to 90% of the net grid energy consumption to form the spot are losses of which 70% are within the electrode caps.<sup>[46]</sup> This means that about 63% of the net energy input needs to be removed from the electrode caps by cooling which equals a cooling energy of 1262 J or a power of 4856 W respectively. For designing the corresponding chiller, it is a common practice to assume a required on time of 20% including a  $\pm 10\%$  variance. As a result, the range of cooling energy to be provided by the chiller is 212–293 J, which corresponds to 817–1125 W of required cooling power. The chiller utilized for cooling the electrode cap is an eChilly3 from WMA with a maximum cooling power of 2810 W and a net power demand of 1.9 kW, which is sufficient to guarantee an effective cooling of the electrode caps.

The evaluation of the energy amount needed for the power source to form the single spot is obtained by corresponding current and voltage measurements using EL 3773 power monitoring

terminals from Beckhoff<sup>[47]</sup> that enable the calculation of the needed power supply including the operation of the welding equipment. As illustrated in **Figure 9**, the effective transient power signal  $P_{\text{eff}}(t)$  is obtained as sum of the power signals of each of the three phases. The integration with respect to the time limits of the ongoing welding process yields the net energy consumption from grid during welding that is 7331 J. However, the operation of the C-gun, the chiller (1.9 kW), and the robot (3 kW) must be regarded for the entire process time of 1.5 s including squeeze, welding and heating time, as well as hold time partitions. The mean value of effective power that is needed from grid for operation of the C-gun was obtained by measurements as shown in **Figure 10** and accounted for 290 W.

Summarizing the total amount of energy consumption from grid to form a single weld spot with a process time of 1.5 s and a weld time of 0.26 s can be listed as follows: 1) Energy input from grid to form spot (average of three measurements): 7331 J. 2) Energy for C-gun (average of three measurements):  $290 \text{ W} \times 1.5 \text{ s} = 435 \text{ J}$ . 3) Energy for cooling electrodes: power supply for chiller:  $1.9 \text{ kW} \times 1.5 \text{ s} = 2850 \text{ J}$ . 4) Energy for operation of the robot:  $3 \text{ kW} \times 1.5 \text{ s} = 4500 \text{ J}$ .

Total electrical energy input from grid:  $7331 + 435 + 2850 + 4500 \text{ J} = 15\,116 \text{ J}$ .

**Welding Process (AC):** The evaluation of the electrical energy amount for realizing a single weld spot in AC mode is done in accordance with the MF-DC mode explained previously and accounts for as follows: 1) Current (averaged three measurements): 8232 A. 2) Voltage (averaged 3 measurements): 1.07 V. 3) Weld time (predefined): 0.26 s. 4) Resulting energy input at the spot:  $8232 \text{ A} \times 1.07 \text{ V} \times 0.26 \text{ s} = 2304 \text{ J}$  (design criterion for chiller to cool the electrode caps). 5) Energy input from grid to form spot (averaged three measurements): 5830 J (**Figure 11**). 6) Energy for C-gun for 1.5 s process time:  $290 \text{ W} \times 1.5 \text{ s} = 435 \text{ J}$ . 7) Energy for cooling electrodes: power supply for chiller:  $1.9 \text{ kW} \times 1.5 \text{ s} = 2850 \text{ J}$ . 8) Energy for operation of the robot:  $3 \text{ kW} \times 1.5 \text{ s} = 4500 \text{ J}$ .

Total electrical energy input from grid:  $5830 + 435 + 2850 + 4500 \text{ J} = 13\,615 \text{ J}$ .

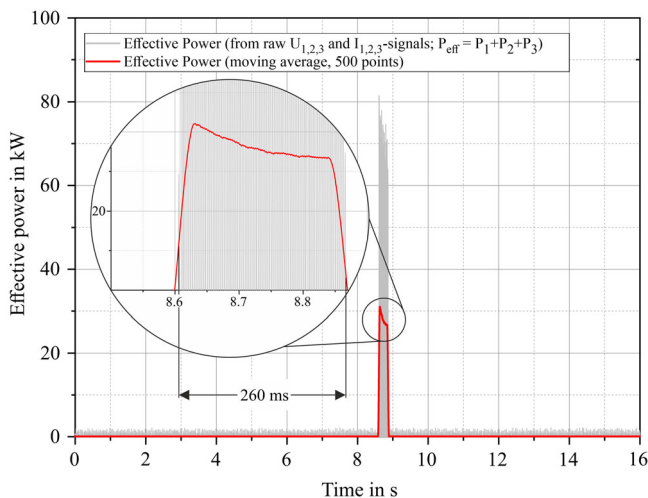


**Figure 9.** Effective power measured during welding of a single spot in mid-frequency direct current (MF-DC) mode.

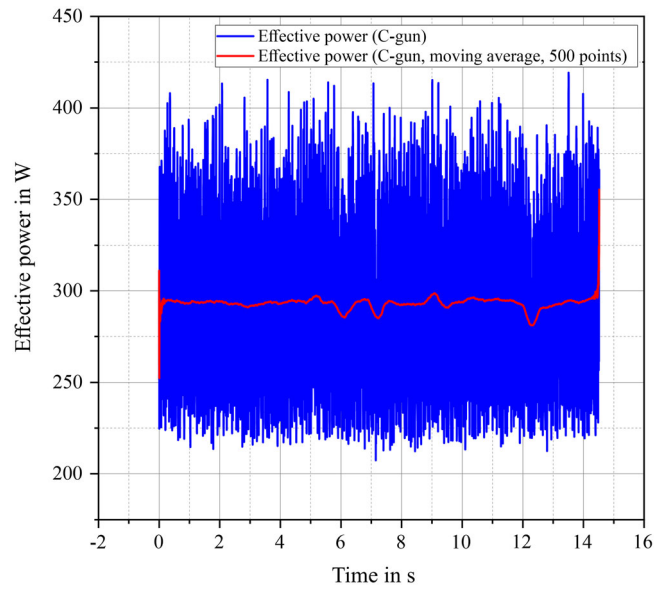


**Figure 10.** Effective power during operation of the C-gun and evaluation of mean value.

**Material Consumption: Base Material Made of DC 05 + ZE Steel Sheets:** The overlap of 12.2 mm (Figure 2), the specimen width of 45 mm, and the sheet thickness of 0.8 mm yield a material amount of 6.89 g if a density of  $7850 \text{ kg m}^{-3}$  is assumed for steel.

**Copper Electrodes:** A single electrode has a weight of 21 g. If a lifetime of 1000 spots per electrode is assumed, this results in a copper waste of  $42 \text{ g}/1000 \text{ spots} = 42 \text{ mg per spot}$ .

#### 4.2.2. Laser Beam Welding: Total Amount of Electrical Energy to Form a Weld of 18 mm Length

With regards to the LBW process parameters that are listed in Table 3, the weld time (laser on) for a weld length of 18 mm

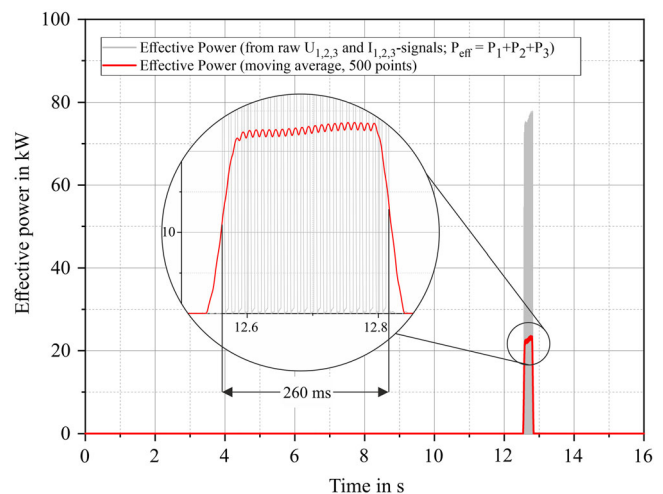


**Figure 11.** Effective power measured during welding of a single spot in AC mode.



accumulates to 0.18 s. Again, the measurement of the effective power over time as shown in **Figure 12** and integration within the time span of welding yield an energy amount of 3354.5 J that corresponds to an effective power needed during welding time of 18.6 kW. It is worth noticing that with regards to the beam power of 4 kW, this correlates with an efficiency of the laser source of  $4 \text{ kW}/18.6 \text{ kW} = 21.5\%$ .

The power demand for the chiller to cool the laser source is 8.5 kW and for cooling the optics additional 2.3 kW are required. For the welding time of 0.18 s, the energy consumption of the chiller follows as  $(8.5 \text{ kW} + 2.3 \text{ kW}) \times 0.18 \text{ s} = 1944 \text{ J}$ . The total energy amount adds up to 1) Energy from grid to operate laser for 0.18 s (average three measurements): 3354.5 J. 2) Energy from grid to operate the chiller for cooling the laser equipment: 1944 J. 3) Energy for robot during welding:  $1.3 \text{ kW} \times 0.18 \text{ s} = 234 \text{ J}$ .

Total electrical energy input from grid:  $3445 + 1944 + 234 \text{ J} = 5532.46 \text{ J}$ .

**Material Consumption: Base Material Made of DC 05 + ZE Steel Sheets:** The overlap of 6 mm (**Figure 3**), the specimen width of 45 mm, and the sheet thickness of 0.8 mm yield a material amount of 3.4 g if a density of  $7850 \text{ kg m}^{-3}$  is assumed for steel.

**Protection Glasses for Optics:** A single protection glass mounted in front of the laser optic has a weight of 96 g. It is assumed that if a part consisting of 20 welds with a total process time of 30 s is manufactured within two 8 h shifts 6 days per week, this requires an exchange of the protection glass every 2 weeks. In that time span, a total number of about 23 040 welded components are realized. Consequently, the waste of protection glasses per part is  $96 \text{ g}/23\,040 \text{ parts} = 4$  and 0.2 mg for a single weld.

**Compressed Air:** The operation of the cross-jet nozzle that protects the laser optics requires compressed air in the range of 7 bar. Considering a volume flow rate of  $30 \text{ L s}^{-1}$ , a total gas flow time of 0.18 s (weld time) + 0.5 s preflow time = 0.68 s, which yields an amount of compressed air of 20.4 L.

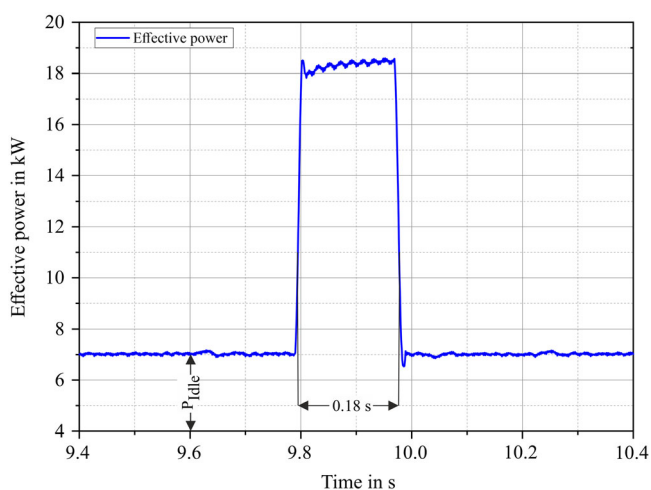


**Figure 12.** Effective power measurement during laser welding (single weld).

### 4.3. Life Cycle Inventory of Cap Profile

#### 4.3.1. Resistance Spot Welding

**Electrical Energy Consumption for MF-DC Mode:** The electrical energy amount for welding the cap profile (**Figure 4**) is governed by the welding time and the idle time of robot motion between the spot welds as described in Section 3.2. Concerning the electrical energy consumption during welding, the results obtained from the analyses of the single spot (see Section 4.2.1) can be extrapolated for the required 20 weld spots per part. This yields an overall energy amount of  $20 \times 15\,116 \text{ J} = 302.32 \text{ kJ}$ .

During the idle phase of 6.9 s (approach and leaving time as well as time for moving between the spots), only the power demand of the chiller (1.9 kW) and the C-gun operation (290 W) has to be taken into account for the two robots:  $2 \times 2.19 \text{ kW} \times 6.9 \text{ s} = 30.22 \text{ kJ}$ . The energy amount of the robots has to be added for the idle time of 6.9 s per robot:  $2 \times 3000 \text{ W} \times 6.9 \text{ s} = 41.4 \text{ kJ}$ . In total, the RSW of the cap profile requires an energy amount of 373.94 kJ.

**Energy Consumption for AC Mode:** The derivation of the energy consumption during AC mode of operation was done accordingly and differs only in the amount for realizing the 20 spot welds:  $20 \times 13\,614 \text{ J} = 272.3 \text{ kJ}$ . The total energy consumption including the C-gun operation, chiller, and both the robots yields a value of 343.92 kJ.

**Material Consumption: Base Material Made of DC 05 + ZE Steel Sheets:** The flange width of 16.6 mm (**Figure 4**), the length of the cap profile of 1000 mm, and the sheet thickness of 0.8 mm yield a material amount of 417 g if a density of  $7850 \text{ kg m}^{-3}$  is assumed for steel.

**Copper Electrodes:** A single electrode has a weight of 21 g. If a lifetime of 1000 spots per electrode is assumed, this results in a copper waste of  $42 \text{ g}/1000 \text{ spots} = 42 \text{ mg}$  per spot and for the manufacturing of the cap profile 840 mg.

#### 4.3.2. Laser Beam Welding

The LBW of the cap profile incorporates two test cases utilizing one robot—the sequential welding of 20 steps (**Figure 5a**) and welding “on-the-fly” as depicted in **Figure 5b**.

**Sequential Welding:** The energy amount of the laser (without cooling) for welding the 20 step welds can be derived from the results for a single laser beam weld presented in Section 4.2.2 and accumulates to  $20 \times 3354.5 \text{ J} = 67.09 \text{ kJ}$ . This corresponds to a total welding time of 1.8 s that requires to add the energy demand of the chiller for cooling the laser and the optics within that time span:  $10.8 \text{ kW} \times 1.8 \text{ s} = 19.44 \text{ kJ}$ .

In addition, within the idle time of 6.3 s, the idle power demand of the chiller (10.8 kW) as well as the idle power of the laser (**Figure 12**) of 7 kW results in a corresponding energy amount. However, two scenarios are considered: 1) During the idle time, only the energy amount of the chiller is considered and the laser is not included as it may be used within a laser network (nearly 100% parallel use time). This results in an energy amount of  $10.8 \text{ kW} \times 6.3 \text{ s} = 68.04 \text{ kJ}$ . 2) The chiller for cooling the laser and optics as well as the idle power of the laser are taken into account during idle which yields  $(10.8 \text{ kW} + 7 \text{ kW}) \times 6.3 \text{ s} = 112.14 \text{ kJ}$ .

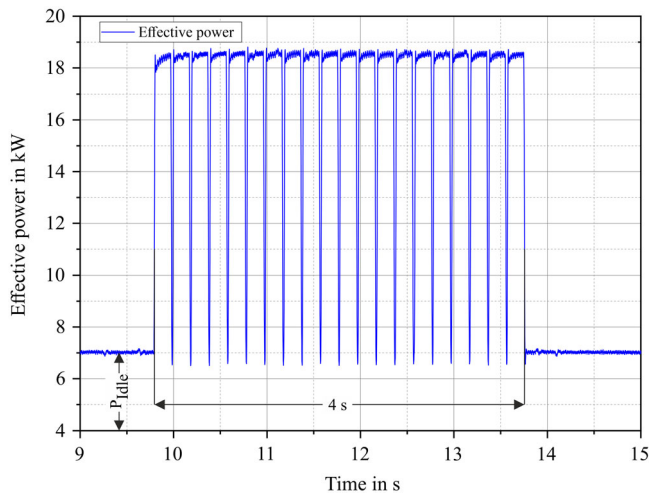


**Figure 13.** Effective power measurement for 20 welding cycles.

The energy amount of the robot includes the total manufacturing time of  $1.8 + 6.3 \text{ s} = 8.1 \text{ s}$  and results in an energy amount of  $1.3 \text{ kW} \times 8.1 \text{ s} = 10.53 \text{ kJ}$ .

The total amount of energy accounts for 86.53 kJ (laser and chiller during welding) + 68.04 kJ (only chiller)/112.14 kJ (laser and chiller) during idle as well as the 10.53 kJ for the robot, which equals 165.1 or 209.2 kJ, respectively.

**Welding “On-The-Fly”:** In case of welding simultaneously “on-the-fly,” the energy amount of the laser was obtained by integrating the transient effective power signal including the 20 welds as shown in **Figure 13**. The integration with regards to the time span of 4 s results in an energy amount for welding of 69.43 kJ.

The idle time (laser-off) is governed by the approach and leaving time of 1.5 s and the laser downtime during moving (0.4 s) and yields 1.9 s. During this time, the idle power demand of the laser correlates with an energy amount of  $7 \text{ kW} \times 1.9 \text{ s} = 13.3 \text{ kJ}$ . During the total manufacturing time of 5.5 s, the power of the chiller makes an energy equivalent of  $10.8 \text{ kW} \times 5.5 \text{ s} = 59.4 \text{ kJ}$ . The energy consumption of the robot must be calculated for the entire process period of 5.5 s and gives a value of  $1.3 \text{ kW} \times 5.5 \text{ s} = 7.15 \text{ kJ}$ . Thus, the total amount of electrical energy needed to produce the 20 laser welds and to operate the chiller for cooling and the robot is 149.3 kJ.

**Material Consumption: Base Material Made of DC 05 + ZE Steel Sheets:** The flange width of 6 mm (Figure 5), the length of the cap profile of 1000 mm, and the sheet thickness of 0.8 mm yield a material amount of 151 g if a density of  $7850 \text{ kg m}^{-3}$  is assumed for steel.

**Protection Glasses for Optics:** A single protection glass mounted in front of the laser optic has a weight of 96 g. It is assumed that if a part consisting of 20 welds with a total process time of 30 s is manufactured within two 8 h shifts 6 days per week, this requires an exchange of the protection glass every two weeks. In that time span, a total number of about 23 040 welded components are realized. Consequently, the waste of protection glasses per part is  $96 \text{ g}/23\,040 \text{ parts} = 4.2 \text{ mg}$ .

**Compressed Air:** The operation of the cross-jet nozzle that protects the laser optics requires compressed air in the range of 7 bar. Considering a volume flow rate of  $30 \text{ L s}^{-1}$ , a total gas flow time of 8.1 s (process time sequential welding) + 0.5 s preflow-time = 8.6 s yields an amount of compressed air of 258 L. In case of welding “on-the-fly,” a total gas flow time of 5.5 s + 0.5 s = 6 s reduces the amount of compressed air to 180 L.

#### 4.4. Life Cycle Impact Analyses of Shear Test Specimens

The resulting inventory analysis that describes the necessary electrical energy and material demands during welding of the shear test specimens is summarized in **Table 6**.

With regards to the electrical energy consumption, it is obvious that the operation of the power sources for RSW as well as for the laser has the main influence. In case of RSW, the share of operating the chiller is in the range of 19–21% whereas the share of the robot electrical energy contribution is 30–33%. The lowest impact on the overall amount of energy consumption originates from the operation of the C-gun and is about 3%.

For LBW, the highest impact of electrical energy consumption is affected by the laser source (60.5%) and the cooling of the laser and the optics (35%). The robot only requires 4.5% of the total energy amount. The difference of the required demand of steel between both the welding processes is mainly technology (design) driven as discussed in Section 3.2 and yields a significant higher material amount in case of RSW.

The considered environmental impact categories (see Section 2) are depicted in **Figure 14** and **15**, which allows a direct comparison of the RSW and the LBW process of the shear test specimens. It is important to note that the material consumption

**Table 6.** Inventory analysis for resistance spot welding of the shear test specimens.

Input/output	Resistance spot welding		Laser beam welding
Electrical energy [J]	AC: 13 614	DC: 15 116	5532.5
	Power source: 42.9%	48.4%	Laser: 60.5%
	Cooling: 20.9%	18.9%	Cooling: 35%
	C-Gun: 3.2%	2.9%	Robot: 4.5%
	Robot: 33%	29.8%	
Material consumption (steel sheet) [g]	6.9		3.4
Compressed air [l]	–		20
Electrode caps (waste) s [mg]	42		–
Protection glass (waste) [mg]	–		0.2

has the most dominant influence for all impact categories followed by the electrical energy consumption. The environmental impact of the laser beam-welded shear test specimen is up to 35% below that of the resistance spot-welded specimen, that is, taking the carbon footprint into account. Moreover, in case of LBW, the consumption of compressed air has a slightly higher impact as the electrical energy. It is interesting to note that the use of protection glasses and electrode caps can be neglected for this scenario.

This simple use case shows that the application of LBW instead of RSW can reduce the environmental impact significantly for all related categories with the same qualitative behavior with regards to the contribution of the considered inputs/outputs like steel, electrical energy, and compressed air. It is worth noticing that despite the low electrical efficiency of the laser beam source of 21.5%, the overall ecological impact is minor in comparison to the consumption of steel but is also significantly lower than the corresponding environmental impact of the electrical energy that is related to the RSW process. Summarizing it can be stated that independent of the welding process

under investigation the use of base material such as steel governs the entire set of environmental impact categories. Consequently, the highest ecological performance of a welding process is directly connected to the material consumption that has to be considered during weld planning, that is, optimization of the joint design.

#### 4.5. Life Cycle Impact Analyses for the Cap Profile

The inventory analysis summarizing the consumption of electrical energy and resources for welding the cap profile of 1000 mm length is given by Table 7. Again, the material consumption is mainly influenced by the different flange widths applied for RSW (16.6 mm) and LBW (6 mm).

For the RSW processes, there occurs only a minor difference in the consumption of electrical energy, which is 344 kJ for the AC mode and 374 kJ for the MF-DC mode. Consequently, the share of cooling (22.5–24.2%), the operation of the C-gun ( $\approx 3.5\%$ ), and the robot action (35–38.2%) do not vary significantly between both the RSW processes.

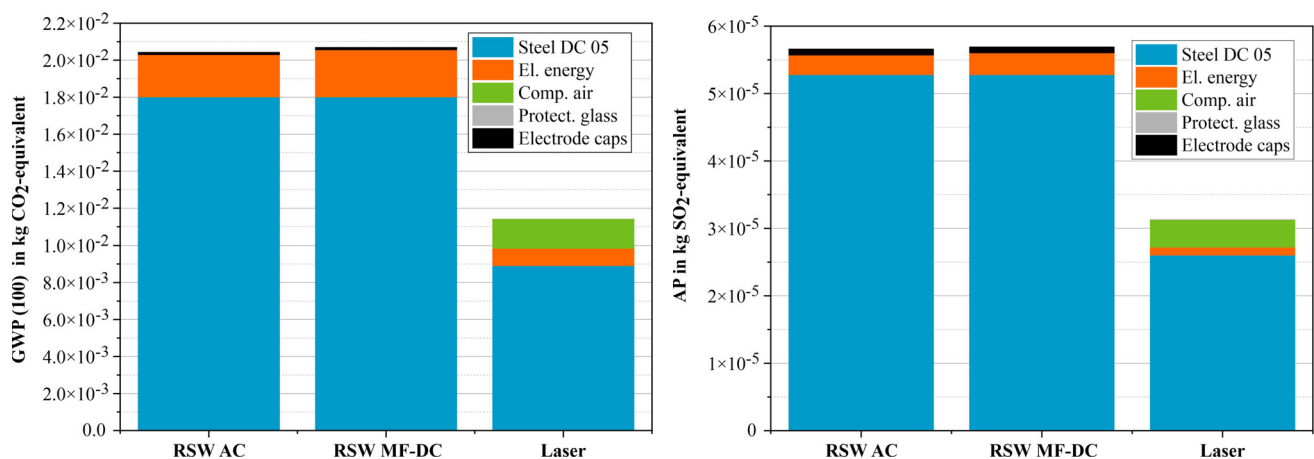


**Figure 14.** Environmental impact categories global warming potential (GWP) (left) and acidification potential (AP) (right) for the shear test specimens.

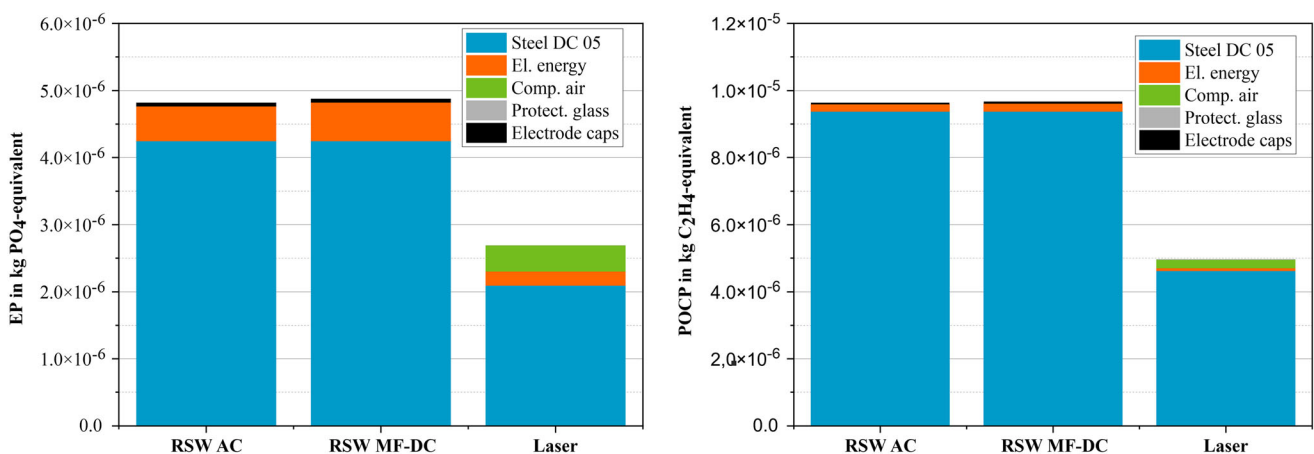


**Figure 15.** Environmental impact categories eutrophication potential (EP) (right) and photochemical ozone creation potential (POCP) (left) for the shear test specimens.

**Table 7.** Inventory for resistance spot welding of the cap profile.

Input/output	Resistance spot welding		Laser beam welding		
	AC	MF-DC	Sequentially (no laser idle/ laser idle)		"on-the-fly"
Electrical energy [kJ]	344	374	165.1	209.2	149.3
	Power source: 33.9%	39%	Laser: 40.6%	53%	55.4%
	Cooling: 24.2%	22.5%	Cooling: 53%	42%	39.8%
	C-gun: 3.7%	3.5%	Robot: 6.4%	5%	4.8%
	Robot: 38.2%	35%			
Steel DC-05 [g]	417			151	
Compressed air [l]	–			258/180	
Electrodes [mg]	840			–	
Protection glass [mg]	–			4.2	

The LBW of the cap profile involved two scenarios as explained in Section 3.2 namely welding sequentially and “on-the-fly” utilizing different scanner optics. As shown in Table 7, the electrical energy amount differs between the contributors of the welding system and accounts between 40.6 and 55.4% for operation of the laser source, 39.8–53% for the chiller used for cooling the laser and the optics and 4.8% and 6.4% for the robot.

It is obvious that the consumption of electrical energy during idle (no welding, only moving of robots for new positioning of laser optic) plays an important role. If the downtime of the laser can be reduced, that is, by integration within a laser network and realizing high power on times, the corresponding required electrical energy is reduced correspondingly up to 21.5%. This agrees with the findings of Kaieler<sup>[16]</sup> and Huang<sup>[15]</sup> who showed that an application of the laser with low downtimes allows an high electrical efficiency. In that context, the lowest amount of electrical energy consumption could be obtained by welding “on-the-fly” during moving of the robot and controlling the laser spot by a programmable scanner optics. The energy saving in comparison to welding sequentially including the idle time of the laser is about 29%. Furthermore, the low downtime of the laser if operated “on-the-fly” results in an reduced manufacturing time,

which decreases the needed volume of compressed air for the cross-jet nozzle of the laser optics and robot use.

Again, the material demand differs significantly between the resistance spot-welded cap profile and the laser beam-welded one due to the different design criteria for the flange widths. In case of LBW, the amount of necessary steel could be reduced by 64%, which is a significant saving.

The corresponding environmental impact categories for welding a cap profile of 1000 mm length are shown in Figure 16 and 17. As for the shear test specimens, the use of steel is of utmost importance for all regarded categories. Accordingly, the resistance spot-welded cap profile has a significantly higher environmental impact of about 272% for all impact categories than the laser beam-welded one. Furthermore, the share of electrical energy consumption on all impact categories is low in comparison to the steel demand.

It must be pointed out that for the three laser beam use cases, the differences in electrical energy consumption only have a minor influence on the environmental impact categories due to the low share of electrical energy versus steel consumption. This means that the mode of laser operation influences the electrical efficiency significantly but has less effect on the ecological impact.

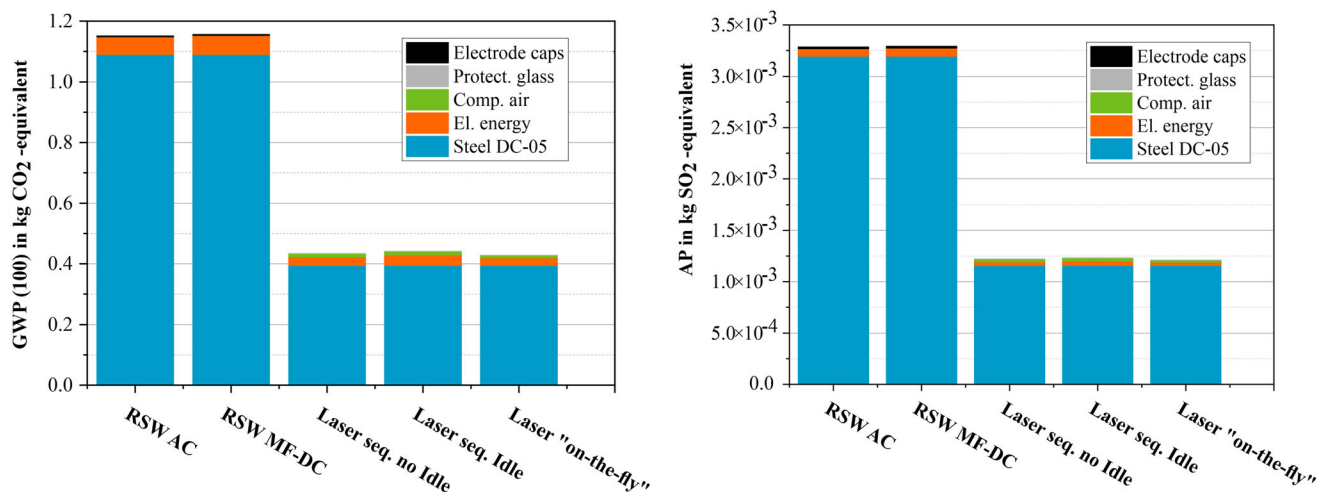


**Figure 16.** Environmental impact categories GWP (left) and AP (right) for the cap profile.

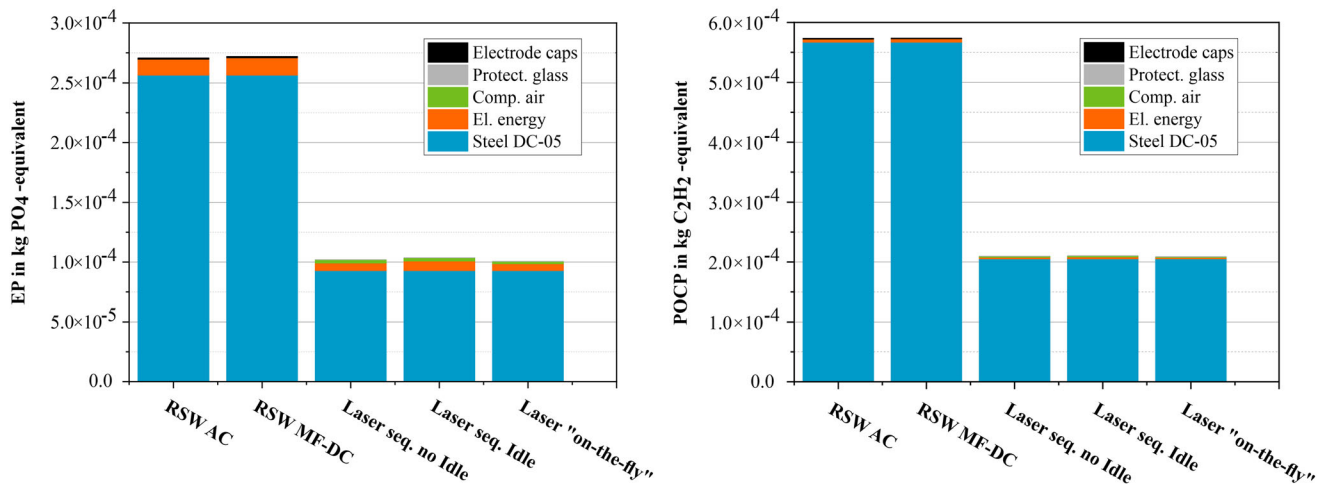


**Figure 17.** Environmental impact categories EP (right) and POCP (left) for the cap profile.

Moreover, in addition to the electrical energy and material usage, the application of cross-jet nozzles and needed compressed air for operation has a visible contribution to the environmental impacts but is not of outmost relevance. The waste of electrode caps in case of RSW as well as protection glasses might be neglected. Therefore, it is found that the analysis of the electrical energy, material, and compressed-air consumption during RSW and LBW allows to provide an appropriate life cycle impact analysis. Again, the importance of the material usage must be stressed and has to be taken into account during weld design, which coincides with the literature by Kaierle et al. and Yilbas et al.<sup>[16,17]</sup> and previous work of Sprosser et al.<sup>[12]</sup>

## 5. Conclusion

This paper presented a methodology for LCIA of fusion welding processes exemplarily for RSW and LBW. The impact categories GWP, EP, AP, and the POCP in accordance with the World Steel Association were found to be adequate to characterize the environmental impact of welding processes.

Furthermore, the ecological efficiency of RSW and LBW has been investigated and compared for two different use cases. The first use case comprises the welding of shear test specimens that fulfilled the requirement of technological consistency between both the welding processes in terms of the mechanical properties of the welds. It could be shown that for LBW, the selected seam length of 18 mm overfulfills the predefined strength criterion by 20%. This results in the potential to reduce the seam length accordingly, which contributes to a decrease of the process time and associated flows as electrical energy and compressed air. Nevertheless, the influence of the material consumption driven by the overlap or flange width is more dominant so that the potential savings in electrical energy may not account for the environmental impacts, respectively. In this context, the better mechanical performance of the fusion joint should be taken as reference.

The RSW and LBW of a cap profile as automotive application scenario represents the second use case. The direct comparison of RSW with LBW offers significant differences in consumption

of electrical energy and material. Moreover, it was demonstrated that for LBW, the total amount of electrical energy consumption decreases significantly if the downtime of the laser is low.

The calculated impact categories showed the material consumption to be the major influencing parameter followed by the electrical energy and compressed air during LBW. The remaining input and output quantities as protection glasses (LBW) as well as electrode caps (RSW) can be neglected, which allows to reduce the effort for the inventory assessment significantly and increases the applicability of life cycle assessment for welding applications as standard design tool.

It is worth noticing that LBW results in up to 60% reduced environmental impacts for both use cases in comparison to the RSW. This is due to the process-specific material consumption governed by the lower sheet overlap and flange width in case of LBW. This design advantage is an important factor for the ecological efficiency and must be considered during weld planning. However, the electrical efficiency of LBW systems might be further enhanced, if the idle time of the laser are managed to be low.

## Acknowledgements

Open Access funding enabled and organized by Projekt DEAL.

## Conflict of Interest

The authors declare no conflict of interest.

## Data Availability Statement

The data that support the findings of this study are available from the corresponding author upon reasonable request.

## Keywords

carbon dioxide footprint, environmental impact categories, laser beam welding, life cycle assessment, resistance spot welding

Received: September 30, 2021

Revised: March 30, 2022

Published online:

- [1] J. Duflou, K. Kellens, W. Dewulf, *CIRP J. Manuf. Sci. Technol.* **2011**, 4, 129.
- [2] H. Ward, M. Burger, Y. Chang, P. Fürstmann, S. Neugebauer, A. Radebach, G. Sproesser, A. Pittner, M. Rethmeier, E. Uhlmann, J. Steckel, *J. Clean. Prod.* **2017**, 163, 154.
- [3] A. Fysikopoulos, D. Anagnostakis, K. Salonitis, G. Chryssoulouris, *Proc. CIRP* **2012**, 3, 477.
- [4] V. Soo, in *Proc. of the AutoCRC 3rd Technical Conf.*, **2014**.
- [5] S. Choudry, S. Steeb, U. Alber, D. Landgrebe, in *7th Int. Conf. on Industrial Technology and Management*, **2018**, <https://doi.org/10.1109/ICITM.2018.8333914>.
- [6] OECD Council Working Party on Shipbuilding (WP6), Environmental and Climate Change Issues in the Shipbuilding Industry, **2010**.
- [7] M. A. Shama, in *Maritime Transportation and Exploitation of Ocean and Coastal Resources*, Vol. 1, **2005**, p. 1751.
- [8] I. Ribeiro, F. Matos, C. Jacinto, H. Salman, G. Cardeal, H. Carvalho, R. Godina, P. Peças, *Sustainability* **2020**, 12, 929.
- [9] Y. Chang, G. Sproesser, S. Neugebauer, K. Wolf, R. Scheumann, A. Pittner, M. Rethmeier, M. Finkbeiner, *Proc. CIRP* **2015**, 26, 293.
- [10] G. Sproesser, Y. Chang, A. Pittner, M. Finkbeiner, M. Rethmeier, *Weld. World* **2017**, 61, 733.
- [11] G. Sproesser, Y. Chang, A. Pittner, M. Finkbeiner, M. Rethmeier, *Int. J. Adv. Manuf. Technol.* **2017**, 91, 3503.
- [12] G. Sproesser, Y. Chang, A. Pittner, M. Finkbeiner, M. Rethmeier, *J. Clean. Prod.* **2015**, 108, 46.
- [13] G. Sproesser, Y. Chang, A. Pittner, M. Finkbeiner, M. Rethmeier, in *Sustainable Manufacturing*, Springer, Cham **2017**, pp. 71–84.
- [14] K. Metha, in *Innovations In Manufacturing For Sustainability. Materials Forming, Machining And Tribology* (Ed: K. Gupta), Springer, Cham **2019**.
- [15] Z. Huang, H. Cao, D. Zeng, *Int. J. Adv. Manuf. Technol.* **2021**, 114, 2433.
- [16] S. Kaieler, M. Dahmen, O. Güdükkurt, in *Proc. SPIE 8065, SPIE Eco-Photonics 2011: Sustainable Design, Manufacturing, and Engineering Workforce Education for a Green Future*, **2011**, p. 80650T.
- [17] B. Yilbas, M. Shaukat, A. Afzal, F. Ashraf, *Opt. Laser Technol.* **2020**, 126, 106064.
- [18] C. Favi, F. Campi, M. Germani, *Int. J. Life Cycle Assess.* **2019**, 24, 2140.
- [19] K. Sangwan, C. Herrmann, P. Egede, V. Bhakar, J. Singer, *Proc. CIRP* **2016**, 48, 62.
- [20] M. Bevilacqua, F. Ciarapica, A. D'Orazio, A. Forcellese, M. Simoncini, *Proc. CIRP* **2017**, 62, 529.
- [21] A. Shrivastava, M. Krones, F. Pfefferkorn, *CIRP J. Manuf. Sci. Technol.* **2015**, 9, 159.
- [22] J. Jamal, B. Darras, H. Kishawy, *Proc. Inst. Mech. Eng. B: J. Eng. Manuf.* **2019**, 234, 501.
- [23] Fronius International, Sustainable Welding: What are the Crucial Factors? <https://www.fronius.com/en/welding-technology/info-centre/magazine/2018/sustainable-welding> (accessed: May 2022).
- [24] K. Epping, H. Zhang, *Sustainability* **2018**, 10, 2.
- [25] C. Favi, F. Campi, M. Germani, *Int. J. Adv. Manuf. Technol.* **2019**, 105, 967.
- [26] J. Duflou, J. Sutherland, D. Dornfeld, C. Herrmann, *CIRP Ann. Manuf. Technol.* **2012**, 61, 587.
- [27] G. Chetan, R. Venkateswara, *J. Clean. Prod.* **2015**, 100, 17.
- [28] L. M. S. Campos, D. A. de Melo Heizen, M. A. Verdinelli, P. A. Cauchick Miguel, *J. Clean. Prod.* **2015**, 99, 286.
- [29] ISO 14040:2006 - Environmental management - Life cycle assessment - Principles and framework, <https://www.iso.org/standard/37456.html>.
- [30] ISO 14044:2006 - Environmental management - Life cycle assessment - Requirements and guidelines, <https://www.iso.org/standard/38498.html>.
- [31] J. Guineé, *Int. J. Lifecycle Assess.* **2001**, 6, 255.
- [32] L. Publications Office European Union, in *Handbook Of International Reference Life Cycle Data System - General Guide For Life Cycle Assessment*, European Commission.
- [33] N. Santero, J. Hendry, *Int. J. Life Cycle Assess.* **2016**, 21, 1543.
- [34] J. Guineé, R. Heijungs, G. Huppes, *Environ. Manag. Health* **2001**, 12, 301.
- [35] *Life Cycle Assessment Methodology Report*, World Steel Association, Brüssel **2011**.
- [36] OpenLCA, <http://www.openlca.org/> (accessed: May 2022).
- [37] GaBi Solutions, <http://www.gabi-software.com/deutsch/index/> (accessed: May 2022).
- [38] DVS Merkblatt 2902-3: Widerstandspunktschweißen von Stählen bis 3 mm Einzeldicke - Konstruktion und Berechnung, Deutscher Verband für Schweißen und verwandte Verfahren e.V., Düsseldorf **2016**.
- [39] SEP 1220-2:2011-08, Testing and Documentation Guideline for the Joinability of Thin Sheet of Steel - Part 2: Resistance Spot Welding, Beuth Publishing, Berlin.
- [40] DVS Merkblatt 3203-4: Laserstrahlschweißen von metallischen Werkstoffen - Nahtvorbereitung und konstruktive Hinweise, Deutscher Verband für Schweißen und verwandte Verfahren e.V., Düsseldorf **2015**.
- [41] Gabi-Dokumentation - Electricity Flow (GER), <http://gabi-documentation-2021.gabi-software.com/xml-data/processes/48ab6f40-203b-4895-8742-9dbdef55e494.xml> (accessed: May 2022).
- [42] Gabi-Dokumentation - Steel ElectroGalvanized (GLO), <http://gabi-documentation-2016.gabi-software.com/xml-data/processes/b0652960-91aa-48a5-a884-977dead71d79.xml> (accessed: May 2022).
- [43] Gabi-Dokumentation - Copper Mix (Global), <http://gabi-documentation-2018.gabi-software.com/xml-data/processes/32cd7ddb-a8d1-402a-ba81-dd6e94e470ff.xml> (accessed: May 2022).
- [44] Gabi-Dokumentation - Compressed Air (EU-28), <http://gabi-documentation-2018.gabi-software.com/xml-data/processes/398d9810-46a2-11dd-ae16-0800200c9a66.xml> (accessed: May 2022).
- [45] Gabi-Dokumentation - Float Flat Glass (Eu-28), <http://gabi-documentation-2018.gabi-software.com/xml-data/processes/641ca70f-fca3-4f27-bac0-b8ad236efaff.xml> (accessed: May 2022).
- [46] DVS Merkblatt 2902-1: Resistance Spot Welding of Steels with Individual Thicknesses up to 3 mm—Overview, Deutscher Verband für Schweißen und verwandte Verfahren e.V., Düsseldorf **2001**.
- [47] Beckhoff Automation GmbH & Co. KG, EL3773 - EtherCAT Terminal, 3-Channel Analog Input, Multi-Function, 500 V AC/DC, 1 A, 16 bit, 10 ksp, Oversampling, <https://www.beckhoff.com/en-us/products/i-o/ethercat-terminals/el3xxx-analog-input/el3773.html> (accessed: May 2022).